DOI: 10.1002/chem.200700501

Mechanisms for the Dehydrogenation of Alkanes on Platinum: Insights Gained from the Reactivity of Gaseous Cluster Cations, Pt_n^+ $n = 1$–21

Christian Adlhart and Einar Uggerud*[a]

Abstract: Rates for the dihydrogen elimination of methane, ethane, and propane with cationic platinum clusters, Pt_n^+ $(1 \le n \le 21)$, were measured under binary collision conditions in a Fourier transform ion cyclotron resonance mass spectrometer (FTICR). The reaction rate for a given cluster, Pt_n^+, follows the trend $k(CH_4) < k(C_2H_6) < k(C_3H_8)$. Methane is particular in the sense that reactivity is highly variable; some clusters ($n = 1$–3, 5–9, 11, 12, 15) are very reactive towards methane, while all other clusters react with low efficiency or not at all. For propane, all clusters react efficiently, while the reactivity of ethane lies in between that of methane and propane. By necessity, dihydrogen elimination of methane occurs according to a 1,1-elimination mechanism. Ethane dehydrogenation takes place according to both a 1,1- and a 1,2-mechanism. The difference between the 1,1- and 1,2-mechanisms is well displayed in specifically increased rates for those clusters that were inefficient in the reaction with methane, as well as in the observed selectivity for H_2, HD, and D_2 elimination in the reaction with $[D_3]$-1,1,1-ethane. Some twofold dihydrogen elimination is observed as well. The outcome of reactions with C_2H_6 in the presence of D_2 demonstrates exchange of all hydrogen atoms in $[Pt_nC_2H_4]^+$ with deuterium atoms. A potential energy diagram with a high barrier for the second H_2 elimination summarizes these observations. For propane twofold dihydrogen elimination is dominating, and for these reactions a far less regiospecific and more random loss of the hydrogens can be inferred, as was demonstrated by the reactions with $[D_6]$-1,1,1,3,3,3-propane.

Keywords: cluster compounds · gas-phase reactions · heterogeneous catalysis · isotope scrambling · platinum

Introduction

Finely dispersed platinum metal is an excellent and widely used catalyst for a number of important reactions, including the contact process for sulphuric acid production, oxidation of ammonia, oxidation of automobile exhaust gases, and hydrogenation of olefins.[1] More recently, platinum has been shown to be useful for oxidative dehydrogenation of ethane and propane (to give olefin and water),[2] and also for partial oxidation of methane to give synthesis gas in connection with the Fisher-Tropsch process.[3] The latter reactions—dehydrogenation/hydrogenation of hydrocarbons, in particular ethane—will be the topic of this paper. We will investigate the mechanism by which molecules interact with the cluster surface during reaction, and how this is linked to the detailed surface structure.

Dissociative chemisorption of ethane on platinum surfaces has been studied by several workers by using a number of experimental approaches including molecular beams,[4–6] spectroscopy,[7,8] low-energy electron diffraction,[9] and microcalorimetry.[10] In addition, there exists a kinetic study as well as density functional theory calculations.[11,12] On the basis of this evidence one envisages two different pathways to dihydrogen elimination, a 1,1- and a 1,2-elimination. After physisorption to the surface, a common C–H activation step leads to an intact ethyl group bonded to one Pt atom and a hydrogen atom bonded to a neighboring Pt atom. A second hydrogen atom may then be transferred to the surface either from the α-carbon or from the β-carbon, corresponding to 1,1- or 1,2-elimination, respectively. The transition structure for the rate determining step of the latter is marginally higher in potential energy than for the former according to DFT calculations.[12] Dihydrogen elimination is accomplished when the two adsorbed hydrogen atoms combine to form a dihydrogen molecule. From the results of an IR reflection absorption spectroscopy measure-

[a] Dr. C. Adlhart, Prof. E. Uggerud
Centre for Theoretical and Computational Chemistry
Department of Chemistry, University of Oslo
P.O. Box 1033 Blindern, 0315 Oslo (Norway)
Fax: (+47) 228-55-441
E-mail: einar.uggerud@kjemi.uio.no

Supporting information for this article is available on the WWW under http://www.chemeurj.org/ or from the author.

ment of a Pt surface in the presence of gaseous ethylene and hydrogen, it was inferred that there are two species present: di-σ-bonded ethylene and ethylidyne, corresponding to the products formed in 1,2- and 1,1-dehydrogenation of ethane, respectively.[13] Isotope exchange in ethane has been studied over platinum surfaces under catalytic conditions, suggesting preferential formation of CH_2DCH_2D over that of CH_3CHD_2.[14]

It was realized very early that the detailed features of the surface could be the key to catalytic activity,[15] a notion which has been strengthened throughout the years.[16] In this respect, metal clusters may be suitable models of the imperfect but reactive sites of a catalyst. It is then of interest to learn how reactivity is related to the molecular and electronic structure of a given cluster. The recent demonstration of catalytic activity of size-selected clusters which were soft-landed on a suitable support is particularly illustrative.[17] Previous studies of naked gas-phase platinum clusters (anionic, neutral, or cationic) have been concentrated on reactions with hydrocarbons[18–21] and oxidation of CO and H_2.[22,23]

On this basis it would be of fundamental interest to conduct a study on the dehydrogenation of ethane by platinum clusters as a function of cluster size. From a limited number of studies it is known that gas-phase platinum clusters dehydrogenate alkanes, including methane.[18,20,21,23] One of these studies includes reactions with ethane but is covering only Pt_n^+ ions with $n=5$.[20] Given the broad interest in and importance of ethane dehydrogenation and ethylene hydrogenation, it would be very valuable to extend this to higher n values and to provide more detail. In this paper we present the results of reactions up to $n=21$. We were also interested in obtaining kinetic data to provide insight into the fascinating mechanistic features of the dihydrogen elimination reaction, namely the questions of 1,1- or 1,2-elimination and to which degree the reaction is reversible. We also include previous results with methane, as well as new results with propane. The present study extends a recent study on ionic rhodium clusters,[24] which is besides platinum a key catalyst for oxidative dehydrogenation.

Results and Discussion

Reactivity of CH_4, C_2H_6, and C_3H_8: Cationic platinum clusters, Pt_n^+ ($n=1$–21), were reacted with methane, ethane, and propane under single-collision conditions. The only reaction observed was dihydrogen elimination. There was no indication for loss of methane. The results are shown in Figure 1. It is highly noticeable that all platinum clusters react rapidly with propane (reaction efficiency, $\phi>0.3$), while reactivity with methane shows a more restricted size dependence and ethane falls in-between. For $n<12$, all clusters except for $n=4$ and 10 react readily with methane. The reactivity of cationic platinum clusters towards methane is very poor for $n=13$ and above, with an exception for $n=15$. We have previously described this to be a binary (on/off) reactivity pattern in the sense that platinum clusters react with methane either with high efficiency ($\phi\approx1$) or not at all.[21] Reactions between cationic platinum clusters and ethane also demonstrate a distinctive size-dependence. All clusters were observed to react and the majority react with high efficiency. The most noticeable exceptions are for $n=13$, 17, and 19 with reaction efficiencies $\phi<0.4$. These three clusters are unreactive towards methane. On the other hand, clusters with $n=4$, 10, 14, 18, 20, and 21, which are all unreactive towards methane have high reaction efficiencies ($\phi>0.8$) with ethane. At this stage of the discussion we will remind ourselves that even small differences in activation energies may account for the large differences in observed reactivity. A difference of about 10 kJ mol^{-1} will determine whether a given reaction has $\phi=1.00$ or <0.01. We will therefore be extremely careful in speculating about underlying differences in molecular and electronic structures.

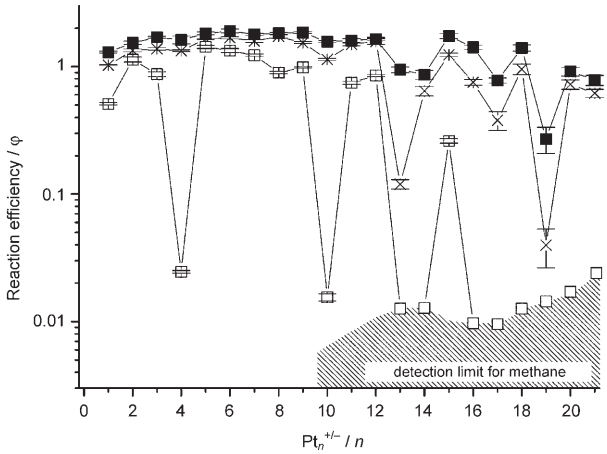

Figure 1. Reaction efficiencies for the reaction of Pt_n^+ with methane, ethane, and propane. The methane data are taken from reference [21]. ■: Pt_n^+ + propane, ×: Pt_n^+ + ethane, □: Pt_n + methane.

The fact that the reactivity of ethane lies in-between that of methane and propane may both reflect differences in C–H bond strengths and a shift in the reaction mechanism. While the dihydrogen elimination of methane by necessity involves a 1,1-elimination mechanism, ethane and propane have additional mechanistic options, at least in principle.

Single and twofold dihydrogen elimination of ethane: Upon reaction with platinum clusters, ethane may lose either one or two dihydrogen molecules:

$$Pt_n^+ + C_2H_6 \rightarrow [Pt_nC_2H_4]^+ + H_2 \quad (1)$$

$$Pt_n^+ + C_2H_6 \rightarrow [Pt_nC_2H_2]^+ + 2H_2 \quad (2)$$

Figure 2 shows which reaction dominates for each cluster size. Except for $n=2$, there is a strong preference for single dihydrogen elimination, although twofold dihydrogen elimination is observed to a variable degree for all clusters in the range of $n=1$–11 (the resolution of our FTICR instrument for ions with m/z: >2200 constraints this type of analysis to

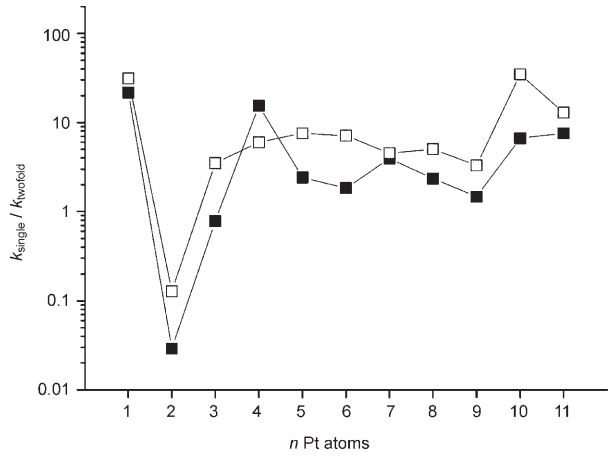

Figure 2. Reaction with ethane. Relative rates for single and twofold dihydrogen elimination. The most significant observation is the dominant twofold dihydrogen elimination for Pt_2^+. ■: branching ratio ethane, □: branching ratio [D_6]ethane.

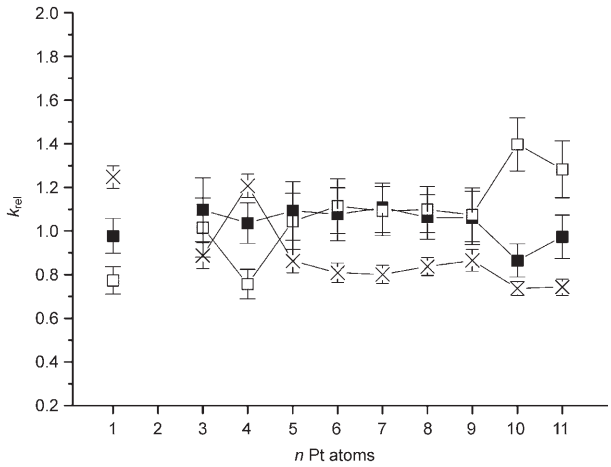

Figure 3. Reaction with [D_3]-1,1,1-ethane. Relative rate constants k_{rel} for single dihydrogen elimination are corrected for the statistical probability of elimination of dihydrogen, 1[$-H_2$]:3[$-$HD]:1[$-D_2$]. The data for $n=2$ are uncertain due to its strong preference for twofold dihydrogen elimination. ■: loss of D_2, ×: loss of HD, □: loss of H_2.

clusters with $n=11$.) Particular reactivity is noticed for $n=2$, for which twofold dihydrogen elimination is dominating and almost complete. This is a fascinating and significant observation, which we cannot explain without explicit knowledge about the electronic configurations of Pt_2^+ and $[Pt_2C_2H_4]^+$. In this context, it may be relevant to refer to the fact that bombardment of a perfect Pt{111} surface with supersonic C_2H_6 gives rise to the loss of one H_2 upon formation of adsorbed $CHCH_3$.[5] The rougher Pt{110}-(1×2) surface is more reactive to the loss of two molecules of H_2.[6] At low temperature, the adsorbed species was shown to be CCH_2 in that case.

Reactions with CH_3CD_3 and the mechanism of ethane dehydrogenation: To investigate the details of the mechanism of the dehydrogenation reaction, we performed reactions with ethane specifically deuterated at one of the methyl groups, namely, [D_3]-1,1,1-ethane. The data are displayed in Figure 3. If the hydrogen and deuterium atoms were completely scrambled prior to dihydrogen loss, the statistically corrected relative rates would have been [$-H_2$]/[$-$HD]/[$-D_2$] 1:3:1. From Figure 3, it is therefore evident that the hydrogen atoms being lost are far from being statistically distributed. On the contrary, the general trend for $n=3$ and 5–11 is a clear preference for loss of H_2 and D_2 compared to loss of HD. The only deviations from this trend are for $n=1$, and 4. The situation is completely different from that observed in reactions between cationic rhodium clusters and ethane, for which dihydrogen elimination could be explained by a specific 1,2-elimination mechanism with a variable degree of isotope scrambling.[24] The only obvious explanation to the present observation is that there is a propensity for 1,1-elimination; this is a key finding. The loss of HD could be due to specific 1,2-elimination. Alternatively, HD elimination or a part of it comes from isotope scrambling prior to dissociation. From the reactions with methane (Figure 1), we noted that the only possible mechanism for methane dehydrogenation is by 1,1-elimination. Extending the alkane chain length by one methylene unit opens up for another alternative, a 1,2-elimination. It is highly likely that both reactions are occurring in parallel. Support for this thought comes from the results of DFT calculations on ethane dehydrogenation on a platinum surface. The estimated activation energies for 1,1-elimination and 1,2-elimination are the same within a few kJ mol^{-1}.[12] It is also worth noticing that the increased efficiency in going from methane to ethane (Figure 1) could be due to the opening of the 1,2-channel. This is particularly significant for the platinum clusters with $n=1$ and 4. These clusters show the highest relative rate for HD elimination—presumably due to 1,2-elimination. At the same time is the reaction efficiency, ϕ, for these two clusters significantly enhanced when enabling the additional 1,2-elimination channel by switching from methane to ethane (about a factor of 6 to 60, Figure 1). The deviation from this trend for Pt_{10}^+ which shows a significantly enhanced reaction efficiency, ϕ, for ethane, but without the preference for HD loss upon reaction with [D_3]-1,1,1-ethane could be due to prior isotope scrambling reactions which will become more important for the larger clusters. The issue of isotope scrambling will be discussed further in the following section on exchange reactions between hydrogen and ethane. As mentioned above, we have concluded that rhodium clusters dehydrogenate ethane by a pure 1,2-elimination mechanism overlaid by a variable degree of H/D scrambling. The nonoccurrence of 1,1-dehydrogenation of ethane by rhodium clusters is consistent with the fact that rhodium clusters do not react with methane.[24]

Although twofold dihydrogen elimination of ethane by platinum clusters only dominates for $n=2$ it is observed for all investigated cluster sizes, typically at about 10% relative occurrence (Figure 2). The results for the reaction with [D_3]-1,1,1-ethane appear surprising at first sight, as from Figure 4, the patterns are very different from what we ob-

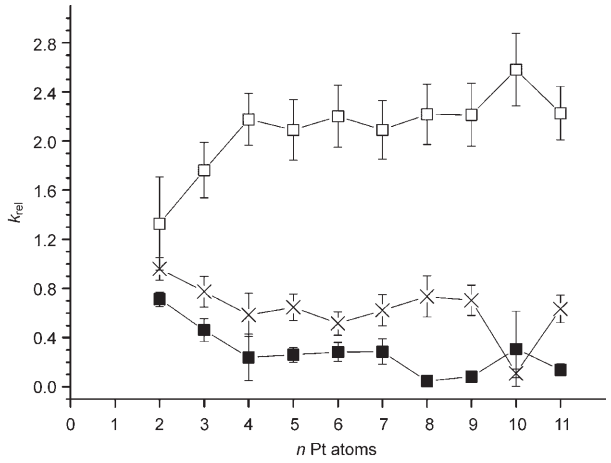

Figure 4. Reaction with $[D_3]$-1,1,1-ethane. Relative rates for twofold dihydrogen elimination are corrected for the statistical probability for elimination of two dihydrogen, 1(D_2 and HD):3(H_2 and D_2 or 2HD):1(H_2 and HD). ■: loss of D_2 and HD, ×: loss of HD and D_2 or 2HD, □: loss of H_2 and HD.

served for single dihydrogen elimination. In particular for $n=4$–9 and 11, there is a strong preference in favor of the combination 3H and 1D, while the complementary 3D and 1H is one order of magnitude less abundant. Loss of 2H and 2D is in-between but closer to the latter. There may be several possible explanations to these significant kinetic isotope effects. However, it is difficult if not impossible to explain this in terms of a rate determining first dihydrogen elimination step(s), as this would imply that the isotopic distribution of Figure 3 which has an equal abundance of H_2 and D_2 losses should be reflected in the product distribution of Figure 4. This is clearly not the case. We also observed that the energy barrier for the second dihydrogen elimination step(s) must be very close to the actual energy content of the majority of the $[Pt_nC_2H_4]^+$ ions formed after the first step. As only 10% of the so-formed $[Pt_nC_2H_4]^+$ ions react further, it is probably slightly above. Under these circumstances, the outcome of a second dihydrogen elimination step will be strongly governed by quantum-mechanical tunneling. If we now assume that only ions that have undergone a 1,2-elimination in the first dihydrogen elimination step will be in the position to react further, we have a simple and rational model. The likelihood for tunneling in the second step is in favor of H_2 to HD, and HD to D_2. This is in agreement with the experimental observations.

Is dehydrogenation reversible? According to this reaction model, the potential energy surface associated with the different $[Pt_nC_2H_4]^+$ species should be quite flat, and it would be of great interest to see to which degree dehydrogenation and hydrogenation are reversible processes. To probe this, we performed experiments in which C_2H_6 and D_2 were added into the cell of the FTICR mass spectrometer simultaneously, but at variable relative concentrations. The results can be divided into two categories, namely clusters with $n=4$ and those with $n>4$. Typical data are reproduced in Figures 5 and 6.

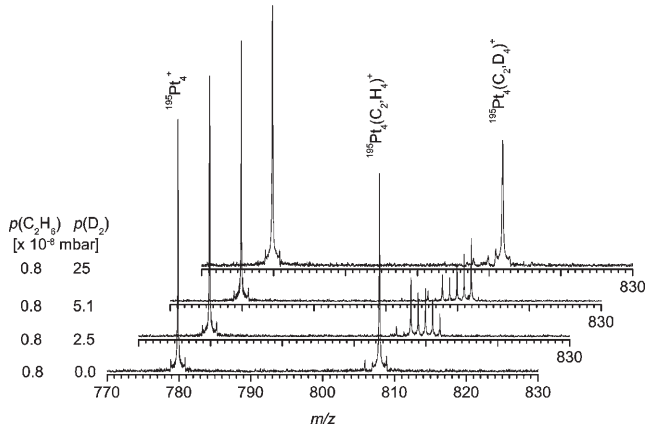

Figure 5. Mixing C_2H_6 and D_2 in the FTICR cell leads to a situation of complete exchange of hydrogen with deuterium in the original $[^{195}Pt_4C_2H_4]^+$ ions.

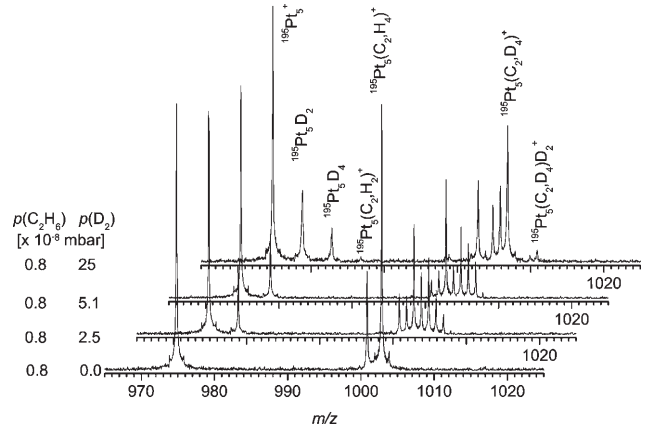

Figure 6. For $n>4$, deuteride clusters $[Pt_nD_m]^+$ are formed ($m=2$, 4). The reaction products with ethane and deuterium are hydride clusters $[Pt_nH_m(C_2H_{2/4})]^+$ as well and not an ethane complex, $[Pt_n(C_2H_6)]^+$. Even though the thermoneutral hydrogen exchange is reversible, the endothermic hydrogenation and ethane elimination is not observed under the experimental conditions.

The evidence for $n=4$ in Figure 5 is clear-cut. In that case, the ultimate reaction product, observed for the $[C_2H_6]$/$[D_2]$ 1:10 mixture, is $[Pt_nC_2D_4]^+$. There is little doubt about how this process occurs. Any $[Pt_nC_2H_4]^+$ present—irrespective of being the result of a 1,1- or a 1,2-elimination—will exchange one or two of its hydrogen atoms with the deuterium atoms of D_2 for each encounter with a D_2 molecule. After a few such encounters, isotope exchange is complete. The intermediates involved in this process are probably of the same structure as those of the initial dihydrogen elimination and the lifetimes of adducts with D_2 are too short to be observed. Clearly, D–D activation by the platinum cluster is an essential requirement for this process.

This rapid isotope exchange could partly be the due to a slight thermodynamic preference for formation of the products resulting from zero-point vibrational energy differences. Assuming standard values of the frequencies of vibrations of the C–H and H–H and normal mass dependent isotope effects, simple calculation shows that exchange of two hydrogen atoms by two deuterium atoms is exothermic by approximately 9 kJ mol^{-1} (see the Supporting Information). Even when we take this detail into account, the experiments clearly indicate low barriers for hydrogen interconversion by a C–H activation mechanism.

From $n=5$ (Figure 6) and above, the picture changes and appears slightly more composite. The two major products upon reaction with ethane are $[Pt_nC_2H_4]^+$ and $[Pt_nC_2H_2]^+$. Interestingly, both exchange their hydrogen atoms with deuterium rapidly and the ultimate isotope exchange products $[Pt_nC_2D_4]^+$ and $[Pt_nC_2D_2]^+$ are clearly seen at higher D_2 concentrations. Besides these, we observe reactant adducts of the type $[Pt_nD_2]^+$ and $[Pt_nD_4]^+$, as well as product adducts, $[Pt_nC_2D_{4+2}]^+$ and $[Pt_nC_2D_{2+2}]^+$. It is somewhat difficult to ascertain the order and identity of all reaction steps involved. It does, however, appear clear that at $[C_2H_6]$:$[D_2]$ 0.8:25 only D_2 monoadducts of the products are visible, while the diadduct of the reactants can be seen. This could be a hint that the reaction with ethane is faster than that with D_2, and that naked platinum clusters react faster than those containing a D_2 unit attached. It is more significant, however, that we note no exchange of the type:

$$[Pt_nC_2D_{4+2}]^+ + C_2H_6 \rightarrow [Pt_nC_2H_6]^+ + C_2D_6 \quad (3)$$

This is a strong indication that $[Pt_nC_2D_{4+2}]^+$ does not contain a unit containing an ethane structure, although we realize this cannot be absolutely proven. It seems most likely that it consists of an $[D_4]$ethylene unit—probably a di-σ-complex and not a π-complex[7]—plus two adsorbed deuterium atoms and that there is a considerable barrier towards activated forms of ethane.

Potential energy diagram for $Pt_n^+ + C_2H_6$: Based on the existing evidence we are now in the position to suggest the qualitative potential energy diagram presented in Figure 7. This diagram incorporates all the basic findings for reactions between cationic platinum clusters and ethane. Firstly, there is a significant barrier—corresponding to the transition state TS_c—for the second dehydrogenation step, being only slightly lower in potential energy than the reactants. Secondly, if the first dihydrogen elimination step gives rise to a loss of energy to H_2 and relative translation exceeding that potential energy difference, then the $[Pt_nC_2H_4]^+$ molecular system will remain on the left side of TS_c. This is more likely to occur for the 1,1-route than for the 1,2-route in agreement with our experimental observations. Translational energy release is intimately linked to the detailed dynamics of the reaction. We note that if the barrier for 1,1-elimination were significantly lower than for the 1,2-elimination, this would explain the results. However, the results above indicate they are close in energy. Thirdly, the barriers for the final leg of the first dihydrogen elimination, denoted $TS_b(1,1)$ and $TS_b(1,2)$, respectively, must be extremely low and of similar order, thereby allowing for the swift incorporation of deuterium observed in the experiments with mixed C_2H_6 and D_2. We will also point out that the left part of the energy diagram is in close agreement with the results of density functional theory calculations.[12]

As already noted, the rates of dihydrogen elimination of propane are generally faster than those for ethane (Figure 1). Furthermore, we observed the close competition for 1,1- and 1,2-eliminations in the reactions with ethane. For propane there is a third option—namely dihydrogen elimination by a 1,3-mechanism. To investigate the mechanistic landscape for dehydrogenation of propane we conducted experiments using $[D_6]$-1,1,1,3,3,3-propane. It is evident that not only is the rate of dihydrogen elimination higher for propane, but the tendency for twofold dihydrogen elimination is more pronounced, Figure 8. In the range investigated ($n=1$–11), only $n=1$, 4, 10, and 11 gave significant single dihydrogen elimination, while the others give primarily twofold dihydrogen elimination. The trend is strengthened by the observation that the clusters that give rise to single dihydrogen elimination are the same that react slowly. For $n=1$, 4, 10, and 11, the same experiments showed that there is very little loss of H_2, while losses of HD and D_2 are of equal abundance for the three latter and

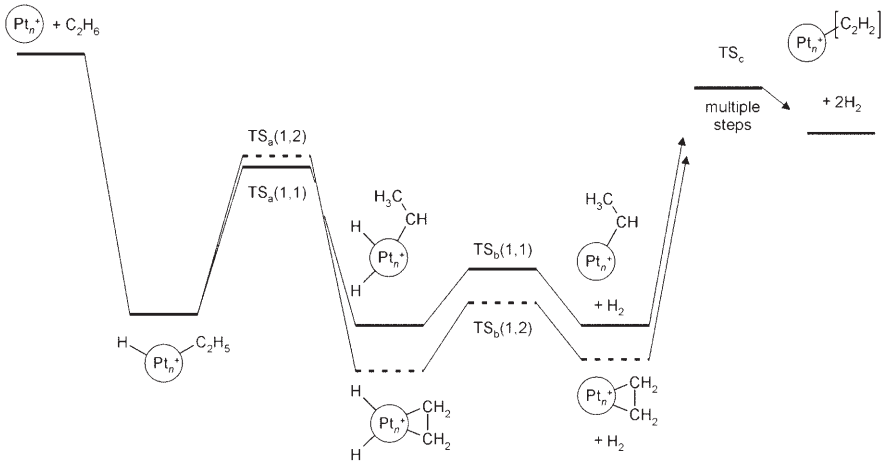

Figure 7. Schematic potential energy diagram for the reaction of cationic Pt-clusters with ethane. There are essentially two routes leading to the loss of dihydrogen; 1,1-elimination (——) and 1,2-elimination (-----). The diagram is only to be understood in qualitative terms, the exact heights of each step will vary with the cluster size.

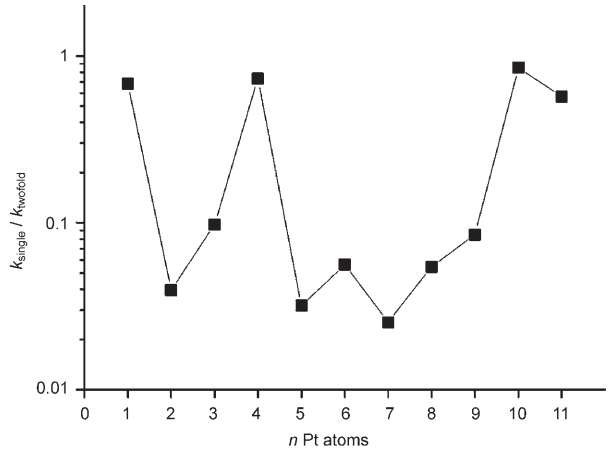

Figure 8. Reaction with $[D_6]$-1,1,1,3,3,3-propane. Relative rates for single and twofold dihydrogen elimination. ■: branching ratio of $[D_6]$-1,1,1,3,3,3-propane.

HD loss is dominating for $n=1$ (Supporting Information). This is different from ethane and precludes 2,2-elimination from the central carbon (would have given H_2 loss), which is remarkable taking into account the fact that the C–H bonds of the central carbon are weaker than the corresponding bonds at the termini. Although we assume that the channel towards 1,3-elimination is open as well, we cannot distinguish it from the 1,1-elimination channel. Our results also demonstrate that there is a shift in favor of 1,2-elimination for propane for these cluster sizes. The clusters that give twofold dihydrogen elimination show a somewhat variable behavior to which degree hydrogen and deuterium atoms are lost (see the Supporting Information). For $n=1$, 2, 8–11 there is preference for loss of H_2 plus D_2 (or 2HD), compared to HD plus D_2 and $2D_2$—the latter two combinations are of approximately the same abundance. The reverse is observed for $n=3$–6, while for $n=7$ all three combinations are equally abundant. Despite these trends, the overall picture for $n>2$ is that all combinations are observed with equal probability within $\pm 20\,\%$. This resembles the situation for cationic rhodium clusters, which appear to dehydrogenate propane in a random fashion, in the sense that hydrogen and deuterium atoms are scrambled prior to dihydrogen elimination. The complexity of the setting does, however, not allow us to discriminate completely between scrambling prior to dihydrogen elimination and a situation with 1,1-, 1,2- and 1,3-eliminations occurring in parallel.

Conclusion

From this study, we have learned that the reactivity of platinum clusters towards alkanes depends both on the cluster size and the size of the alkane. The reactivity pattern for alkanes is regular with $k(CH_4)<k(C_2H_6)<k(C_3H_8)$. The only reaction is dihydrogen elimination (single or twofold). While methane shows high selectivity in its reactivity (fast reaction for $n=1$–3, 5–9, 11, 12, and 15 and no/slow reaction for $n=4$, 10, 13, 14, and 16–21), propane is essentially reactive for all values of n with efficiencies, ϕ, above 0.8 per collision. Ethane lies in-between methane and propane for all cluster sizes. The isotope labeling experiments indicate a gradual shift in reaction mechanism in going from methane to propane via ethane. While methane displays only 1,1-elimination, an additional (minor) 1,2-elimination mechanism is observed for most cluster sizes for the reaction with ethane. For propane, 1,2-elimination seems to dominate. The outcome of reactions with C_2H_6 in the presence of D_2 demonstrates rapid exchange of all hydrogens in $[Pt_nC_2H_4]^+$ with deuterium. A potential energy diagram summarizes these observations.

The strong link between the present study and the use of platinum as an industrial catalyst for hydrogenation and dehydrogenation was emphasized in the introduction. During the experiments discussed above, the close relationship between dehydrogenation on cationic platinum clusters and the corresponding reactions on platinum surfaces has become evident. In the future—with better tools available for structure determination of gas-phase clusters and more reliable quantum chemical methods—it will hopefully be possible to understand the underlying causes and clarify the connection between the observed reactivity trends for clusters in terms of size and geometry and the local structure of reactive surfaces.

Experimental Section

General: The experiments were performed with a Fourier transform ion cyclotron resonance (FTICR) mass spectrometer, Bruker Apex 47e (Bruker Daltonics, MA, USA), with a supplementary cluster ion source chamber with additional pumping attached to the standard source chamber. The experimental setup is of the same design as used by Berg and coworkers and has been described elsewhere.[25] Here a description of the operational techniques and conditions specific to the present study will be given.

Platinum cluster cations were generated by pulsed laser vaporization of a rotating platinum disk. We used isotopically enriched ^{195}Pt (97.3 %, Oak Ridge National Laboratories). A hot plasma was produced by focusing the second harmonic (532 nm) of a PL8020 Nd:YAG laser (Continuum, CA, USA, 20 Hz, 6–12 mJ per 5 ns pulse, spot size 0.1–0.2 mm) on the target. The plasma was subsequently cooled and clustered by coexpansion with a short pulse of helium carrier gas through a confining channel (35 mm, 2 mm i.d.). The helium gas (99.9999 %, Aga, Norway) was provided by a custom-built piezoelectronic valve (30 μs opening time, backing pressure 30–40 bar). As both ions and neutrals are made in the process, further ionization becomes unnecessary. The cluster ions were accelerated downstream from a 410 μm skimmer, transferred into the high field region of the 4.7 T superconducting magnet, decelerated and trapped in the ICRcell. The cluster size distribution is mainly determined by the backing pressure, the laser intensity, and the delay time between the laser pulse and the opening of the piezoelectronic valve. Due to the time-of-flight limitations imposed by the instrument duty cycle, the width of the cluster distribution is limited. To increase the signal intensity, platinum clusters were accumulated by 40 repetitive cluster generation and transfer cycles.

Deuterium (99.998 %, Hydro Gas, Norway), ethane (99.9 %), propane (99.95 %), $[D_6]$ethane (99 atom %), $[D_3]$-1,1,1-ethane (99 atom %), $[D_2]$-2,2-propane (99 atom %), and $[D_6]$-1,1,1,3,3,3-propane (98 atom %, all Icon Isotopes, USA) were dispensed into the FTICR cell through a leak

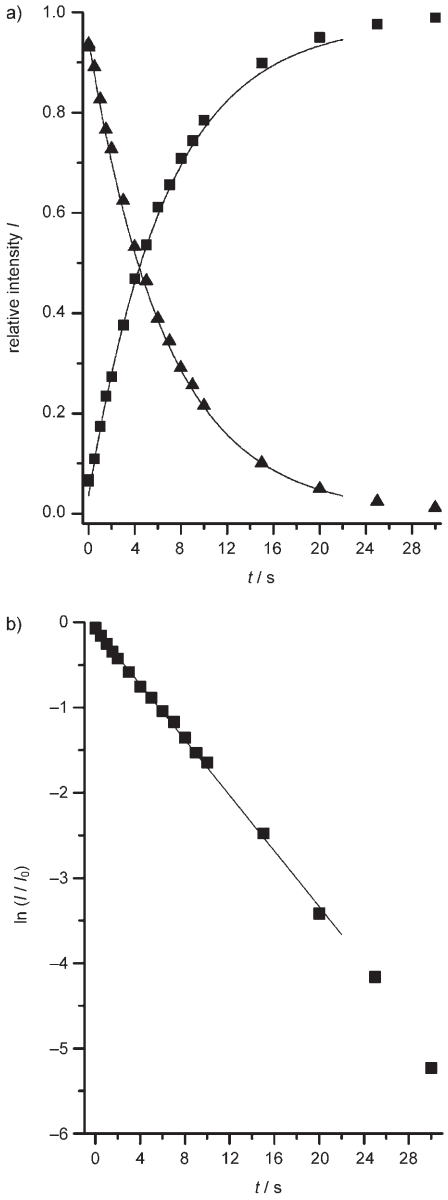

Figure 9. Reaction of Pt^+ with methane after additional thermalization with argon. a) relative intensities of the reactant and product ion at variable reaction time, t_r. Each reaction time represents an independent experiment. To avoid any bias from slight drifts in the experimental conditions, the ordering of t_r was chosen randomly. ▲: Pt^+, ■: $[PtC_2H_4]^+$. b) Plot of the natural logarithm of the normalized cluster ion intensities against t_r and linear fit (0 to 20 s) to obtain pseudo-first-order bimolecular rate constants.

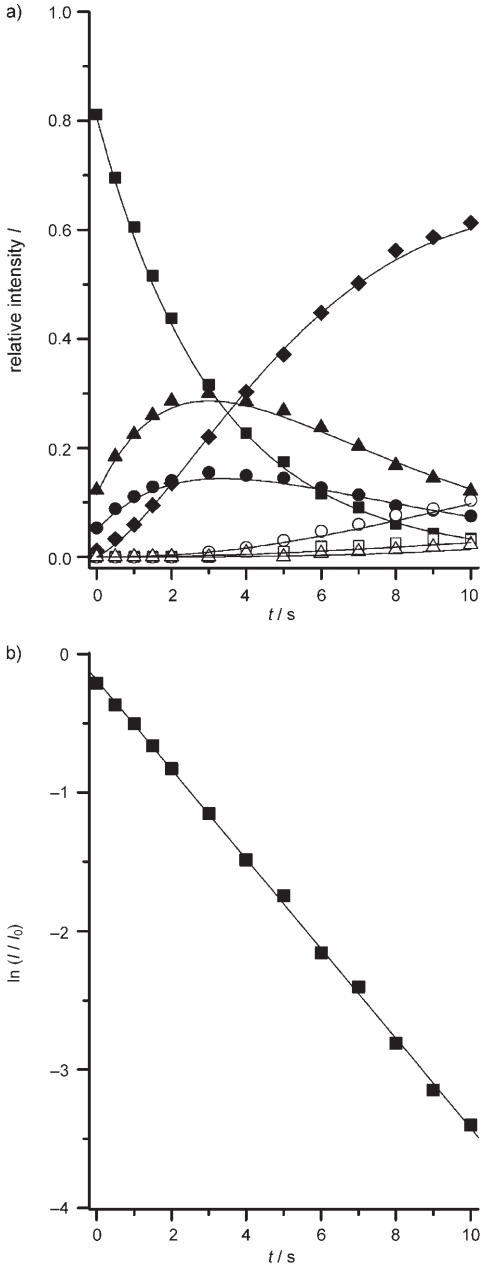

Figure 10. Reaction of Pt_6^+ with ethane. Left panel: relative intensities of the reactant and product ions at variable t_r. Right panel: Plot of the natural logarithm of the normalized cluster ion intensities against t_r and linear fit (0 to 10 s) to obtain pseudo-first-order bimolecular rate constants. ■: Pt_6^+, ●: $[Pt_6C_2H_2]^+$, ▲: $[PtC_2H_4]^+$, ◆: $Pt_6C_4H_8$, □: $[Pt_6C_6H_8]^+$, ○: $[Pt_6C_6H_{10}]^+$, △: $[Pt_6C_8H_{12}]^+$.

valve. During the experiments, the pressure in the cell was raised from the base value of $\approx 3\times10^{-10}$ mbar to partial pressures of the hydrocarbons estimated to approximately 5×10^{-9} to 5×10^{-8} mbar. The substrate pressure was read out by means of a cold cathode ion gauge which was calibrated by using the reaction of $NH_3^{+\bullet}$ (generated externally by EI) + $NH_3 \rightarrow NH_4^+ + NH_2^\bullet$, $k = 2.2\times10^{-9}$ cm^3 mol^{-1} s^{-1}[26] and corrected by relative sensitivity factors of $R(NH_3) = 1.12$, $R(H_2) = 0.59$, $R(CH_4) = 1.23$, $R(C_2H_6) = 1.91$, and $R(C_3H_8) = 2.56$.[27] The sensitivity factors had been calculated with the respective polarizabilities $\alpha(NH_3) = 2.81$, $\alpha(H_2) = 0.8042$, $\alpha(CH_4) = 2.593$, $\alpha(C_2H_6) = 4.47$, and $\alpha(C_3H_8) = 6.29\times10^{-24}$ cm^{-3}. Approximate gas mixtures were prepared in situ by introducing the gases through independent leak valves.

Rate constants for the reactions of each cluster were determined directly from the total cluster distributions without prior isolation. Mass spectra were recorded after a variable reaction time, t_r, thereby giving the product ion distribution with time. Pseudo-first-order bimolecular rate constants for the total consumption of the platinum cluster cations were taken from the slope of the straight lines obtained by plotting the natural logarithm of the normalized cluster ion intensities against t_r. The intensities were normalized against the total sum of ion intensities pertaining to each specific reactant cluster. To determine reaction rates without interference of potential decomposition products from larger clusters, separate experiments were performed in which cluster cations of one specific

size (m/z value) were isolated and subjected to the hydrocarbons or to dihydrogen. Isolation was achieved by ejecting undesired ions from the cell by using correlated frequency sweeps[28] and in some cases by using additional single frequency shots. These isolation experiments were performed for each cluster size and we could thereby confirm that there were no interfering cluster decomposition reactions within the timescale of our experiments, when using the total cluster distributions without prior isolation to obtain the kinetic data. The detection limit for slow reactions (Figure 1) is mainly the result of reactions of the naked platinum clusters and platinum cluster products with background oxygen, for which the reaction chronology is not unambiguously determined.

The uncertainty of the absolute rates is typically $\pm 40\,\%$, but relative rates are very precise. Relative errors are given at the 95 % confidence level. Reactions were observed until 90 % consumption of the parent cluster ion with the exception of some slow reactions as indicated in the text. Rates are given in terms of reaction efficiencies, ϕ, which are the observed rates divided by the theoretical collisional rates (see the Supporting Information). The latter were obtained by the parameterized model of Su and Chesnavich.[29] Our experimental reaction efficiencies of >1.00 are explained by the fact that Su's and Chesnavich's model underestimates real collision rates to some extent, as surface charge distribution is neglected.[30] Branching ratios for the primary products were obtained from pseudo-first-order kinetic fits to the experimental data extracted at early reaction times before secondary products became significant ($<5\,\%$ relative to the most intense peak).

To avoid contributions from long-living excited states, absolute rate constants of the monatomic platinum cation were determined after thermalization for 3 s followed by isolation. Thermalization was achieved upon introduction of a short pulse of argon (peak pressure 1×10^{-6} mbar, ≈ 40 collisions). Thermalization of higher clusters prior to reaction is confirmed by the straight lines of the cluster ion intensities against time (vide infra; Figures 9 and 10). Positive or negative curviture in the plots would have indicated cooling or heating of nonthermalized clusters through collisional or radiative processes during the reactions. This is clearly not the case. We found that additional cooling through argon shots is only required to some extent for the monatomic platinum cations, while larger clusters thermalized efficiently through collisional and radiative processes as well as internal conversion, etc. during the transfer from the source region into the FTICR cell.

Acknowledgements

The authors wish to thank the NFR (Norwegian Research Council) for financial support through the KOSK program for a postdoctoral fellowship for C.A.

[1] F. Zaera, G. A. Somorjai, *J. Am. Chem. Soc.* **1984**, *106*, 2288.
[2] F. Donsi, S. Cimino, R. Pirone, G. Russo, D. Sanfilippo, *Catal. Today* **2005**, *106*, 72; F. Donsi, S. Cimino, A. Di Benedetto, R. Pirone, G. Russo, *Catal. Today* **2005**, *105*, 551; B. Silberova, M. Fathi, A. Holmen, *Appl. Catal. A* **2004**, *276*, 17.
[3] S. C. Tsang, J. B. Claridge, M. L. H. Green, *Catal. Today* **1995**, *23*, 3.
[4] M. C. McMaster, S. L. M. Schroeder, R. J. Madix, *Surf. Sci.* **1993**, *297*, 253; F. W. Jason, A. K. Michael, J. M. Robert, *J. Chem. Phys.* **2000**, *112*, 396.
[5] D. J. Oakes, H. E. Newell, F. J. M. Rutten, M. R. S. McCoustra, M. A. Chesters, *Chem. Phys. Lett.* **1996**, *253*, 123; H. E. Newell, M. R. S. McCoustra, M. A. Chesters, C. D. L. Cruz, *J. Chem. Soc. Faraday Trans.* **1998**, *94*, 3695.
[6] J. J. W. Harris, V. Fiorin, C. T. Campbell, D. A. King, *J. Phys. Chem. B* **2005**, *109*, 4069.
[7] P. Cremer, C. Stanners, J. W. Niemantsverdriet, Y. R. Shen, G. Somorjai, *Surf. Sci.* **1995**, *328*, 111.
[8] P. S. Cremer, X. Su, Y. R. Shen, G. A. Somorjai, *J. Am. Chem. Soc.* **1996**, *118*, 2942.
[9] U. Starke, A. Barbieri, N. Materer, M. A. Van Hove, G. A. Somorjai, *Surf. Sci.* **1993**, *286*, 1.
[10] Y. Y. Yeo, A. Stuck, C. E. Wartnaby, D. A. King, *Chem. Phys. Lett.* **1996**, *259*, 28.
[11] R. M. Watwe, B. E. Spiewak, R. D. Cortright, J. A. Dumesic, *J. Catal.* **1998**, *180*, 184; R. M. Watwe, R. D. Cortright, J. K. Norskov, J. A. Dumesic, *J. Phys. Chem. B* **2000**, *104*, 2299.
[12] A. T. Anghel, D. J. Wales, S. J. Jenkins, D. A. King, *Chem. Phys. Lett.* **2005**, *413*, 289.
[13] T. Ohtani, J. Kubota, J. N. Kondo, C. Hirose, K. Domen, *J. Phys. Chem. B* **1999**, *103*, 4562.
[14] A. Loaiza, D. Borchardt, F. Zaera, *Spectrochim. Acta Part A* **1997**, *53 A*, 2481; A. Loaiza, M. Xu, F. Zaera, *J. Catal.* **1996**, *159*, 127; A. Loaiza, F. Zaera, *J. Am. Soc. Mass Spectrom.* **2004**, *15*, 1366.
[15] H. S. Taylor, *Proc. R. Soc. London Ser. A* **1925**, *108*, 105; H. S. Taylor, *Z. Elektrochem. Angew. Phys. Chem.* **1929**, *35*, 542.
[16] G. A. Somorjai, *Introduction to Surface Chemistry and Catalysis*, Wiley, New York, **1994**; G. A. Somorjai, K. McCrea, *Appl. Catal. A* **2001**, *222*, 3.
[17] S. Abbet, K. Judai, L. Klinger, U. Heiz, *Pure Appl. Chem.* **2002**, *74*, 1527.
[18] D. J. Trevor, R. L. Whetten, D. M. Cox, A. Kaldor, *J. Am. Chem. Soc.* **1985**, *107*, 518; T. F. Magnera, D. E. David, J. Michl, *J. Am. Chem. Soc.* **1987**, *109*, 936; D. J. Trevor, D. M. Cox, A. Kaldor, *J. Am. Chem. Soc.* **1990**, *112*, 3742; G. S. Jackson, F. M. White, C. L. Hammill, R. J. Clark, A. G. Marshall, *J. Am. Chem. Soc.* **1997**, *119*, 7567; U. Achatz, C. Berg, S. Joos, B. S. Fox, M. K. Beyer, G. Niedner-Schatteburg, V. E. Bondybey, *Chem. Phys. Lett.* **2000**, *320*, 53; K. Koszinowski, D. Schroeder, H. Schwarz, *J. Phys. Chem. A* **2003**, *107*, 4999.
[19] A. Kaldor, D. M. Cox, *J. Chem. Soc. Faraday Trans.* **1990**, *86*, 2459.
[20] T. Hanmura, M. Ichihashi, T. Kondow, *J. Phys. Chem. A* **2002**, *106*, 11465.
[21] C. Adlhart, E. Uggerud, *Chem. Commun.* **2006**, 2581.
[22] P. A. Hintz, K. M. Ervin, *J. Chem. Phys.* **1994**, *100*, 5715; P. A. Hintz, K. M. Ervin, *J. Chem. Phys.* **1995**, *103*, 7897; Y. Shi, K. M. Ervin, *J. Chem. Phys.* **1998**, *108*, 1757; M. Andersson, A. Rosén, *J. Chem. Phys.* **2002**, *117*, 7051; O. P. Balaj, I. Balteanu, T. T. J. Rossteuscher, M. K. Beyer, V. E. Bondybey, *Angew. Chem.* **2004**, *116*, 6681; *Angew. Chem. Int. Ed.* **2004**, *43*, 6519; I. Balteanu, O. Petru Balaj, M. K. Beyer, V. E. Bondybey, *Phys. Chem. Chem. Phys.* **2004**, *6*, 2910.
[23] G. Kummerlöwe, I. Balteanu, Z. Sun, O. P. Balaj, V. E. Bondybey, M. K. Beyer, *Int. J. Mass Spectrom.* **2006**, *254*, 183.
[24] G. Albert, C. Berg, M. Beyer, U. Achatz, S. Joos, G. Niedner-Schatteburg and V. E. Bondybey. *Chem. Phys. Lett.* **1997**, *268*, 235–241, C. Adlhart, E. Uggerud, *J. Chem. Phys.* **2005**, *123*, 214709; C. Adlhart, E. Uggerud, *Int. J. Mass Spectrom.* **2006**, *249–250*, 191; I. Balteanu, O. P. Balaj, M. K. Beyer and V. E. Bondybey, *Int. J. Mass Spectrom.* **2006**, *255–256*, 71–75.
[25] C. Berg, T. Schindler, G. Niedner-Schatteburg, V. E. Bondybey, *J. Chem. Phys.* **1995**, *102*, 4870; Å. M. L. Øiestad, E. Uggerud, *Chem. Phys.* **2000**, *262*, 169.
[26] Y. Ikezoe, S. Matsuoka, M. Takebe, A. Viggiano, Gas Phase Ion-Molecule Reaction Rate Constants Through 1986, Maruzen, Tokyo, **1987**.
[27] J. E. Bartmess, R. M. Georgiadis, *Vacuum* **1983**, *33*, 149.
[28] L. J. de Koning, N. M. M. Nibbering, S. L. van Orden, F. H. Laukien, *Int. J. Mass Spectrom. Ion Proc.* **1997**, *165*/166, 209.
[29] T. Su, W. J. Chesnavich, *J. Chem. Phys.* **1982**, *76*, 5183.
[30] G. Kummerlöwe, M. K. Beyer, *Int. J. Mass Spectrom.* **2005**, *244*, 84.

Received: March 31, 2007
Published online: May 31, 2007

